Ruthenium(II) Ammine and Hydrazine Complexes with $[N(Ph_2PQ)_2]^-$ (Q = S, Se) Ligands

Qian-Feng Zhang,[†,‡] Hegen Zheng,[†,‡] Wai-Yeung Wong,[§] Wing-Tak Wong,[∥] and Wa-Hung Leung*[,†]

Departments of Chemistry, The Hong Kong University of Science and Technology, Clear Water Bay, Kowloon, Hong Kong, People's Republic of China, The Hong Kong Baptist University, Kowloon Tong, Kowloon, Hong Kong, People's Republic of China, and The University of Hong Kong, Pokfulam Road, Hong Kong, People's Republic of China, and Coordination Chemistry Institute and Department of Chemistry, Nanjing University, Nanjing 210093, People's Republic of China

Received March 15, 2000

Reactions of coordinatively unsaturated $Ru[N(Ph_2PQ)_2]_2(PPh_3)$ (Q = S (**1**), Se (**2**)) with pyridine (py), SO_2, and NH_3 afford the corresponding 18e adducts $Ru[N(Ph_2PQ)_2]_2(PPh_3)(L)$ (Q = S, L = NH_3 (**5**); Q = Se, L = py (**3**), SO_2 (**4**), NH_3 (**6**)). The molecular structures of complexes **2** and **6** are determined. The geometry around Ru in **2** is pseudo square pyramidal with PPh_3 occupying the apical position, while that in **6** is pseudooctahedral with PPh_3 and NH_3 mutually cis. The Ru−P distances in **2** and **6** are 2.2025(11) and 2.2778(11) Å, respectively. The Ru−N bond length in **6** is 2.185(3) Å. Treatment of **1** or **2** with substituted hydrazines L or NH_2OH yields the respective adducts $Ru[N(Ph_2PQ)_2]_2(PPh_3)(L)$ (Q = S, L = NH_2NH_2 (**12**), *t*-$BuNHNH_2$ (**14**), 1-aminopiperidine ($C_5H_{10}NNH_2$) (**15**); Q = Se, L = $PhCONHNH_2$ (**7**), $PhNHNH_2$ (**8**), NH_2OH (**9**), *t*-$BuNHNH_2$ (**10**), $C_5H_{10}NNH_2$ (**11**), NH_2NH_2 (**13**)), which are isolated as mixtures of their trans and cis isomers. The structures of *cis*-**14** and *cis*-**15** are characterized by X-ray crystallography. In both molecular structures, the ruthenium adopts a pseudooctahedral arrangement with PPh_3 and hydrazine mutually cis. The Ru−N bond lengths in *cis*-**14**·CH_2Cl_2 and *cis*-**15** are 2.152(3) and 2.101(3) Å, respectively. The Ru−N−N bond angles in *cis*-**14**·CH_2Cl_2 and *cis*-**15** are 120.5(4) and 129.0(2)°, respectively. Treatment of **1** with hydrazine monohydrate leads to the isolation of yellow **5** and red *trans*-$Ru[N(Ph_2PS)_2]_2(NH_3)(H_2O)$ (**16**), which are characterized by mass spectrometry, ^1H NMR spectroscopy, and elemental analyses. The geometry around ruthenium in **16** is pseudooctahedral with the NH_3 and H_2O ligands mutually trans. The Ru−O and Ru−N bond distances are 2.118(4) and 2.142(6) Å, respectively. Oxidation reactions of the above ruthenium hydrazine complexes are also studied.

Introduction

Transition-metal diazene (NH═NH) and hydrazine complexes are of current interest because these species are believed to be possible intermediates in the biological reduction of nitrogen.[1] The structural identification of the resting state of the FeMo cofactor of *nitrogenases* as an $[MoFe_7S_9]$ cluster core inspires new speculation on the molecular mechanism of biological nitrogen fixation.[2] Recently, Coucouvanis and co-workers demonstrated that an Fe/Mo/S cubane-like cluster is capable of catalyzing the disproportionation of N_2H_4 to NH_3, suggesting that the Mo center in the FeMo cofactor may play a role in nitrogen fixation, at least in the reduction of hydrazine.[3] The most extensively studied hydrazine complexes are those containing d^6 metal centers such as Mo(0), W(0), Re(I), Ru(II), and Os(II).[4−7] Diazene, which is highly reactive in its free state, can be stabilized by coordination to transition metals. Sellmann and co-workers isolated binuclear Ru(II) diazene complexes with polydentate thiolate ligands by air oxidation of the Ru(II) hydrazine precursors. The solid-state structures of these bi-

* Corresponding author. Email: chleung@ust.hk.
† The Hong Kong University of Science and Technology;
‡ Nanjing University.
§ The Hong Kong Baptist University.
∥ The University of Hong Kong.

(1) (a) Chatt, J.; Richards, R. L. In *The Chemistry and Biochemistry of Nitrogen Fixation*; Postgate, J. R., Ed.; Plenum: London, 1971. (b) Zollinger, H. *Diazo Chemistry II*; VCH: Weinheim, Germany, 1995. (c) Hidai, M.; Mizobe, Y. *Chem. Rev.* **1995**, *95*, 1115. (d) Sutton, D. *Chem. Rev.* **1993**, *93*, 935. (e) Sellmann, D. *Angew. Chem., Int. Ed. Engl.* **1993**, *32*, 64. (f) Kisch, H.; Holzmerier, P. *Adv. Organomet. Chem.* **1992**, *34*, 67.

(2) (a) Chan, M. K.; Kim, J.; Rees, D. C. *Science* **1993**, *260*, 792. (b) Kim, J.; Woo, D.; Rees, D. C. *Biochemistry* **1993**, *32*, 7104.

(3) (a) Demadis, K. D.; Coucouvanis, D. *Inorg. Chem.* **1995**, *34*, 3658. (b) Demadis, K. D.; Campana, C. F.; Coucouvanis, D. *J. Am. Chem. Soc.* **1995**, *117*, 7832.

(4) (a) Sellmann, D.; Sutter, J. In *Transition Metal Sulfur Chemistry*: *Biological and Industrial Significance*; Stiefel, E. I., Matsumoto, K., Eds.; ACS Symposium Series 653; American Chemical Society: Washington, DC, 1996; p 101 and references therein. (b) Nugent, W. A.; Haymore, B. L. *Coord. Chem. Rev.* **1980**, *31*, 123. (c) Schrock, R. R.; Glassman, T. E.; Vale, M. G. *J. Am. Chem. Soc.* **1991**, *113*, 725. (d) Sellmann, D.; Lechner, P.; Knoch, F.; Moll, M. *J. Am. Chem. Soc.* **1992**, *114*, 922. (e) Heaton, B. T.; Jacob, C.; Page, P. *Coord. Chem. Rev.* **1996**, *154*, 193.

(5) (a) Southern, J. S.; Hillhouse, G. L. *J. Am. Chem. Soc.* **1997**, *119*, 12406. (b) Cheng, T.-Y.; Perters, J. C.; Hillhouse, G. L. *J. Am. Chem. Soc.* **1994**, *116*, 204. (c) Cheng, T.-Y.; Ponce, A.; Rheingold, A. L.; Hillhouse, G. L. *Angew. Chem., Int. Ed. Engl.* **1994**, *33*, 657. (d) Smith, M. R., III; Cheng, T.-Y.; Hillhouse, G. L. *J. Am. Chem. Soc.* **1993**, *115*, 8638.

(6) (a) Sellmann, D.; Kunstmann, H.; Knoch, F.; Moll, M. *Inorg. Chem.* **1988**, *27*, 4183. (b) Sellmann, D.; Soglowek, W.; Knoch, F.; Moll, M. *Angew. Chem., Int. Ed. Engl.* **1989**, *28*, 1272. (c) Sellmann, D.; Soglowek, W.; Knoch, F.; Ritter, G.; Dengler, J. *Inorg. Chem.* **1992**, *31*, 3711. (d) Sellmann, D.; Käppler, J.; Moll, M.; Knoch, F. *Inorg. Chem.* **1993**, *32*, 960. (e) Sellmann, D.; Friedrich, H.; Knoch, F.; Moll, M. *Z. Naturforsch.* **1994**, *49B*, 660. (f) Sellmann, D.; Gottschalk-Gaudig, T.; Heinemann, F. W. *Inorg. Chem.* **1998**, *37*, 3982. (g) Sellmann, D.; Engl, K.; Heinemann, F. W. *Eur. J. Inorg. Chem.* **2000**, 423. (h) Sellmann, D.; Engl, K.; Heinemann, F. W.; Sieler, J. *Eur. J. Inorg. Chem.* **2000**, 1079.

10.1021/ic000291c CCC: $19.00
Published on Web 10/26/2000

nuclear Ru diazene complexes reveal that the bridging diazene ligand is stabilized by intramolecular S···H−N hydrogen bonds.[6] Mononuclear diazene complexes of W, Ru, and Os have also been prepared by Pb(IV) oxidation of the respective hydrazine precursors.[5] To our knowledge, no Ru hydrazine complexes with selenide ligands are known to date. To this end, we set out to prepare Ru hydrazine complexes containing chelating sulfide and selenide ligands and studied their oxidation reactions. Of particular interest are Ru complexes with sterically bulky iminobis(phosphinechalcogenide) ligands $(R_2PQ)_2NH$ (R = Ph, *i*-Pr; Q = S, Se). Metal complexes with the bidentate chelating ligands $[N(R_2PQ)_2]^-$ (Q = O, S, Se; R = alkyl or phenyl) (e.g., structure **I**) are known to exhibit interesting stereochemistry.[8]

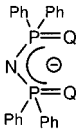

$[N(Ph_2PQ)_2]^-$ (Q = S, Se)

I

The geometry of the $M[N(PR_2E)_2]$ metallacycle is very flexible and can be tuned by judicious choice of the peripheral alkyl groups and the chalcogenides at two ends of the diphosphazene fragment.[8] Due to strong metal−chalcogenide interactions in the six-membered $M[N(R_2PQ)_2]$ ring, it is possible to generate and stabilize highly reactive unsaturated molecular fragments $M[N(PR_2E)_2]_2$, which can be used for the activation of small molecules. Woollins and co-workers first isolated Ru cluster compounds with $[N(R_2PQ)_2]^-$ by reactions of $(R_2PQ)_2NH$ with $Ru_3(CO)_{12}$.[9] Recently, we reported the isolation of 16e $Ru[N(R_2PS)_2]_2(PPh_3)$ (R = Ph, *i*-Pr), which show weak Ru−C−H agostic interactions in the solid state. These coordinatively unsaturated Ru/S complexes form adducts readily with pyridine and are capable of activating H_2 and SO_2.[10] Five-coordinate $Ru[N(R_2PS)_2]_2(=CHPh)$ was found to be an active catalyst for the ring-opening polymerization of norbornene.[11] In this paper, we describe the syntheses of Ru hydrazine complexes with $[N(Ph_2PQ)_2]^-$ (Q = S, or Se) and the oxidation reactions of these complexes.

Experimental Section

General Considerations. Solvents were purified by standard procedures and distilled prior to use. All manipulations, unless otherwise stated, were carried out under nitrogen using standard Schlenk techniques. $Ru[N(Ph_2PS)_2]_2(PPh_3)$ (**1**) was prepared according to our previously reported method.[10] $K[N(Ph_2PQ)_2]$ (Q = S, Se) were synthesized by deprotonation of $HN(Ph_2PQ)_2$[12] with potassium *tert*-butoxide in methanol, and $Ru(PPh_3)_3Cl_2$[13] was obtained from the reaction $RuCl_3 \cdot xH_2O$ and PPh_3 in MeOH. A 35% solution of NH_2NH_2 in water, hydrazine monohydrate $N_2H_4 \cdot H_2O$, *t*-$BuNHNH_2$, $PhNHNH_2$, $PhCONHNH_2$, NH_2OH, and 1-aminopiperidine ($C_5H_{10}NNH_2$) were purchased from Aldrich. Other reagents were obtained from commercial sources and used as received.

NMR spectra were recorded on a Bruker ALX 300 spectrometer operating at 300 and 121.5 MHz for ^1H and ^{31}P, respectively. Chemical shifts (δ, ppm) are reported with reference to $SiMe_4$ (^1H) and 85% H_3PO_4 (^{31}P). Infrared spectra were recorded on a Perkin-Elmer 16 PC FT-IR spectrophotometer, and mass spectra were obtained on a Finnigan TSQ 7000 spectrometer. Cyclic voltammetry was performed with a Princeton Applied Research (PAR) model 273A potentiostat. The working and reference electrodes were glassy carbon and $Ag/AgNO_3$ (0.1 M in acetonitrile) electrodes, respectively. Potentials are reported with reference to the ferrocenium−ferrocene ($Cp_2Fe^{+/0}$) couple. Elemental analyses were performed by Medac Ltd., Surrey, U.K.

Preparation of $Ru[N(Ph_2PSe)_2]_2(PPh_3)$, 2. A mixture of $Ru(PPh_3)_3Cl_2$ (0.50 mg, 0.52 mmol) and $K[N(Ph_2PSe)_2]$ (0.58 mg, 1.00 mmol) in tetrahydrofuran (THF) (40 mL) was stirred overnight at room temperature, during which there was a color change from brown to dark green. The solvent was pumped off, and the residue was washed with Et_2O. Recrystallization from CH_2Cl_2/Et_2O afforded dark-green block-shaped crystals of **2**, which were suitable for X-ray diffraction study. Yield: 0.52 g, 69%. ^1H NMR ($CDCl_3$): δ 7.33−7.94 (m, phenyl protons). $^{31}P\{^1H\}$ NMR ($CDCl_3$): δ 34.53 (s, $N(Ph_2PSe)_2$), 23.19 (s, PPh_3). IR (KBr; cm^{-1}): 1172(s) and 800(s) [$\nu(P_2N)$], 532(vs) [ν(P=Se)]. MS (FAB): *m*/*z* 1448 (M^+), 1187 ($M^+ - PPh_3$). $E_{1/2}$ (CH_2Cl_2; V): −0.17 [Ru(III/II)]. Anal. Calcd for $C_{66}H_{55}N_2P_5Se_4Ru$: C, 54.75; H, 3.83; N, 1.94. Found: C, 55.23; H, 4.14; N, 1.92.

Preparation of *trans*-$Ru[N(Ph_2PSe)_2]_2(PPh_3)(py)$ (py = Pyridine), *trans*-3. Excess py was added to a well-stirred solution of **2** (80 mg, 0.055 mmol) in THF (15 mL). The green solution immediately became yellow, and a large amount of orange solid precipitated. After 15 min of stirring, the solvent was removed and the solid product was isolated. Recrystallization from CH_2Cl_2/Et_2O afforded orange needles of **3**. Yield: 79 mg, 94%. ^1H NMR ($CDCl_3$): δ 7.30−7.55 (m, 45H, phenyl protons), 7.66−7.76 (br, 5H, py). $^{31}P\{^1H\}$ NMR ($CDCl_3$): δ 22.45 (d, $^2J_{P-P}$ = 3.4 Hz, $N(Ph_2PSe)_2$), 45.19 (m, PPh_3). IR (KBr; cm^{-1}): 1480(s) [ν(C=N)], 1174(s) and 807(s) [$\nu(P_2N)$], 534(vs) [ν(P=Se)]. MS (FAB): *m*/*z* 1448 ($M^+ - py$), 1187 ($M^+ - py - PPh_3 + 1$). $E_{1/2}$ (CH_2Cl_2; V): −0.21 [Ru(III/II)]. Anal. Calcd for $C_{71}H_{60}N_3P_5Se_4Ru$: C, 55.84; H, 3.96; N, 2.75. Found: C, 55.80; H, 4.00; N, 2.64.

Preparation of *cis*- and *trans*-$Ru[N(Ph_2PSe)_2]_2(PPh_3)(SO_2)$, *cis*- and *trans*-4. Through a solution of **2** (90 mg, 0.062 mmol) in THF (20 mL) was bubbled SO_2(g) for 30 s, during which the color of the solution changed from green to orange. The resulting mixture was stirred for 1 h at room temperature and then evaporated to dryness, after which the residue was washed with hexane. Recrystallization from CH_2Cl_2/hexane afforded red rhombohedral crystals. Yield: 64 mg (68%). The product was found to consist of cis and trans forms in solution. ^1H NMR ($CDCl_3$): δ 6.53−7.76 (m, phenyl protons). $^{31}P\{^1H\}$ NMR ($CDCl_3$): *trans*-**4** δ 25.80 (d, $^2J_{P-P}$ = 12 Hz, $N(Ph_2Se)_2$), 55.38 (m, PPh_3); *cis*-**4** δ 19.42, 23.11, 45.13, 47.26, 55.98 (all multiplets). IR (KBr; cm^{-1}): 1214(m) and 810(s) [$\nu(P_2N)$], 531(vs) [ν(P=Se)], 1017(vs), 996(vs) [ν(S=O)]. MS (FAB): *m*/*z* 1448 ($M^+ - SO_2$). Anal. Calcd for $C_{66}H_{55}N_3O_2P_5SSe_4Ru$: C, 52.43; H, 3.67; N, 1.85. Found: C, 52.38; H, 3.92; N, 2.02.

Preparations of *cis*- and *trans*-$Ru[N(Ph_2PQ)_2]_2(PPh_3)(NH_3)$ (Q = S)5), Se (6)). These complexes were prepared similarly to **4** by treating **1** and **2** with NH_3(g). The products were isolated as yellow (for **5**) and red (for **6**) crystals. Both were found to exist as their cis and trans forms in solution.

(7) (a) Hough, J. J.; Singleton, E. *J. Chem. Soc., Chem. Commun*. **1972**, 371. (b) Ashworth, T. V.; Nolte, M. J.; Singleton, E. *J. Chem. Soc., Dalton Trans*. **1978**, 1040. (c) Blum, L.; Williams, I. D.; Schrock, R. R. *J. Am. Chem. Soc*. **1984**, *106*, 8316. (d) Collman, J. P.; Hutchison, J. E.; Lopez, M. A.; Guilard, R.; Reed, R. A. *J. Am. Chem. Soc*. **1991**, *113*, 2794. (e) Kawano, M.; Hoshino, C.; Matsumoto, K. *Inorg. Chem*. **1992**, *31*, 5158. (f) Coia, G. M.; Devenney, M.; White, P. S.; Meyer, T. J. *Inorg. Chem*. **1997**, *36*, 2341. (g) Furuhashi, T.; Kawano, M.; Koide, Y.; Somazawa, R.; Matsumoto, K. *Inorg. Chem*. **1999**, *38*, 109. (h) Sun, X.-R.; Huang, J.-S.; Cheung, K.-K.; Che, C.-M. *Inorg. Chem*. **2000**, *39*, 820.

(8) (a) Ly, T. Q.; Woollins, J. D. *Coord. Chem. Rev*. **1998**, *176*, 451. (b) Cupertino, D.; Keyte, R.; Slawin, A. M. Z.; Williams, D. J.; Woollins, J. D. *Inorg. Chem*. **1996**, *35*, 2695. (c) Bhattacharyya, P.; Slawin, A. M. Z.; Williams, D. J.; Woollins, J. D. *J. Chem. Soc., Dalton Trans*. **1995**, 3189.

(9) Alexandra, M. Z. S.; Smith, M. B.; Woollins, J. D. *J. Chem. Soc., Dalton Trans*. **1997**, 1877.

(10) Leung, W.-H.; Zheng, H.; Chim, J. L. C.; Chan, J.; Wong, W.-T.; Williams, I. D. *J. Chem. Soc., Dalton Trans*. **2000**, 423.

(11) Leung, W.-H.; Lau, K.-K.; Zhang, Q.-F.; Wong, W.-T.; Tang, B.-Z. *Organometallics* **2000**, *19*, 2084.

(12) (a) Wang, F. T.; Najdzionek, J.; Leneker, K. L.; Wasserman, H.; Braitsch, D. M. *Inorg. Synth. Met-Org. Chem*. **1978**, *8*, 120. (b) Bhattacharyya, P.; Novosad, J.; Phillips, J.; Slawin, A. M. Z.; Williams, D. J.; Woollins, J. D. *J. Chem. Soc., Dalton Trans*. **1995**, 1607.

(13) Stephenson, T. A.; Wilkinson, G. *J. Inorg. Nucl. Chem*. **1966**, *28*, 945.

Yield of **5**: 35 mg, 35%. ^{1}H NMR ($CDCl_3$): δ 1.00 (br s, 3H, NH_3), 2.6 (br s, 3H, NH_3), 7.07−8.13 (m, 110H, phenyl protons). $^{31}P\{^1H\}$ NMR ($CDCl_3$): *trans*-**5** δ 37.89 (d, $^2J_{P-P}$ = 3.6 Hz, $N(Ph_2PS)_2$), 46.53 (m, PPh_3); *cis*-**5**, δ 36.14, 38.58, 38.92, 40.56, 50.28 (all multiplets). IR (KBr; cm^{-1}): 3335(m) [ν(N−H)], 1178(s) and 800(s) [$\nu(P_2N)$], 565-(vs) [ν(P═S)]. MS (FAB): *m*/*z* 1260 ($M^+ - NH_3$). $E_{1/2}$ (CH_2Cl_2; V): −0.31 [Ru(III/II)]. Anal. Calcd for $C_{66}H_{58}N_3P_5S_4Ru$: C, 61.4; H, 4.5; N, 3.1. Found: C, 62.1; H, 4.5; N, 3.3.

Yield of **6**: 59 mg, 62%. ^{1}H NMR ($CDCl_3$): δ 0.99 (br s, 3H, NH_3), 2.71 (br s, 3H, NH_3), 6.81−7.83 (m, 110H, phenyl protons). $^{31}P\{^1H\}$ NMR ($CDCl_3$): *trans*-**6** δ 21.12 (d, $^2J_{P-P}$ = 3.5 Hz, $N(Ph_2PSe)_2$), 48.83 (m, PPh_3); *cis*-**6** δ 18.51, 22.04, 22.73, 27.30, 51.64 (all multiplets). IR (KBr; cm^{-1}): 3336(m) [ν(N−H)], 1201(s) and 804(s) [$\nu(P_2N)$], 532-(vs) [ν(P═Se)]. MS (FAB): *m*/*z* 1448 ($M^+ - NH_3$), 1187 ($M^+ - NH_3 - PPh_3$). $E_{1/2}$ (CH_2Cl_2; V): −0.21 [Ru(III/II)]. Anal. Calcd for $C_{66}H_{58}N_3P_5Se_4Ru$: C, 54.11; H, 3.99; N, 2.87. Found: C, 54.38; H, 4.17; N, 2.92.

Preparation of *cis*- and *trans*-Ru[N(Ph$_2$PSe)$_2$]$_2$(PPh$_3$)(PhCONHNH$_2$), *cis*- and *trans*-7. To a solution of **2** (100 mg, 0.069 mmol) in THF (25 mL) was added $PhCONHNH_2$ (10 mg, 0.070 mmol) in THF (5 mL), and the mixture was stirred at room temperature for 3 h, during which there was a color change from green to dark orange. The solvent was pumped off, and the residue was washed with hexane. Recrystallization from CH_2Cl_2/hexane afforded orange crystals. Yield: 58 mg, 53%. The product was found to consist of cis and trans forms of **7** in solution. ^{1}H NMR ($CDCl_3$): δ 4.87 (m, $RuNH_2$), 6.72−7.65 (m, phenyl protons), 7.90 (t, NH). $^{31}P\{^1H\}$ NMR ($CDCl_3$): *trans*-**7** δ 22.67 (d, $^2J_{P-P}$ = 6.4 Hz, $N(Ph_2PSe)_2$), 62.66 (m, PPh_3); *cis*-**7** δ 20.76, 21.81, 23.65, 25.13, 20.76 (all multiplets). IR (KBr; cm^{-1}): 3227(w), 3211-(w) [ν(N−H)], 1632(s) [ν(C═O)], 1206(vs) and 798(s) [$\nu(P_2N)$], 536-(vs) [ν(P═Se)]. $E_{1/2}$ (CH_2Cl_2; V): −0.19 [Ru(III/II)]. Anal. Calcd for $C_{73}H_{63}N_4OP_5Se_4Ru$: C, 55.35; H, 4.01; N, 3.54. Found: C, 55.25; H, 4.15; N, 3.82.

Preparations of *cis*- and *trans*-Ru[N(Ph$_2$PSe)$_2$]$_2$(PPh$_3$)(L) (L = PhNHNH$_2$ (8), NH$_2$OH (9), *t*-BuNHNH$_2$ (10), C$_5$H$_{10}$NNH$_2$ (11)). These complexes were prepared similarly to **7** by using $PhNHNH_2$, NH_2OH, *t*-$BuNHNH_2$, and $C_5H_{10}NNH_2$, respectively, instead of $PhCONHNH_2$. The products were found to exist as their cis and trans forms in solutions.

Yield of **8**: 50 mg, 46%. ^{1}H NMR ($CDCl_3$): δ 6.81−7.83 (m, phenyl protons); NH signals not assigned. $^{31}P\{^1H\}$ NMR ($CDCl_3$): *trans*-**8** δ 21.10 (d, $^2J_{P-P}$ = 6.8 Hz, $N(Ph_2PSe)_2$), 48.62 (m, PPh_3); *cis*-**8** δ 18.39, 22.10, 23.51, 27.34, 52.01 (all multiplets). IR (KBr; cm^{-1}): 3347(w), 3252(w) [ν(N−H)], 1206(s) and 794(s) [$\nu(P_2N)$], 532(vs) [ν(P═Se)]. $E_{1/2}$ (CH_2Cl_2; V): −0.20 [Ru(III/II)]. Anal. Calcd for $C_{72}H_{63}N_4P_5Se_4Ru\cdot H_2O$: C, 54.90; H, 4.13; N, 3.56. Found: C, 54.56; H, 4.41; N, 3.45.

Yield of **9**: 55 mg, 54%. ^{1}H NMR ($CDCl_3$): δ 2.81 (br s, $RuNH_2$), 6.83−7.75 (m, phenyl protons), 8.27 (br s, OH). $^{31}P\{^1H\}$ NMR ($CDCl_3$): *trans*-**9** δ 22.67 (d, $^2J_{P-P}$ = 6.4 Hz, $N(Ph_2PSe)_2$), 64.23 (m, PPh_3); *cis*-**9** δ 21.06, 21.81, 23.65, 24.84, 25.13 (all multiplets). IR (Nujol, cm^{-1}): 3450(br) [ν(O−H)], 3269(w) [ν(N−H)], 1230(s), 1176-(m) and 797(s) [$\nu(P_2N)$], 532(vs) [ν(P═Se)]. $E_{1/2}$ (CH_2Cl_2; V): −0.19 [Ru(III/II)]. Anal. Calcd for $C_{66}H_{58}N_3OP_5Se_4Ru$: C, 53.53; H, 3.95; N, 2.84. Found: C, 54.59; H, 4.33; N, 2.73.

Yield of **10**: 60 mg, 47%. ^{1}H NMR ($CDCl_3$): δ 1.40 (s, 9H, *t*-Bu), 2.35 (br s, NH), 4.81 (br s, $RuNH_2$), 6.87−7.71 (m, 55H, phenyl protons). $^{31}P\{^1H\}$ NMR ($CDCl_3$): *trans*-**10** δ 21.16 (d, $^2J_{P-P}$ = 3.3 Hz, $N(Ph_2PSe)_2$), 48.62 (m, PPh_3); *cis*-**10** δ 18.72, 21.91, 22.65, 27.85, 50.13 (all multiplets). IR (KBr; cm^{-1}): 3348(w) [ν(N−H)], 1202(s), 1152(m) and 784(s) [$\nu(P_2N)$], 532(vs) [ν(P═Se)]. MS (FAB): *m*/*z* 1449 ($M^+ - t$-$BuNHNH_2$), 1186 ($M^+ - t$-$BuNHNH_2 - PPh_3$). $E_{1/2}$ (CH_2Cl_2; V): −0.26 [Ru(III/II)]. Anal. Calcd for $C_{70}H_{67}N_4P_5Se_4Ru$: C, 54.73; H, 4.40; N, 3.65. Found: C, 55.12; H, 4.32; N, 3.55.

Yield of **11**: 69 mg, 54%. ^{1}H NMR ($CDCl_3$): δ 1.27 (d, $2H_\gamma$, C_5H_{10}), 1.67 (d, $4H_\beta$, C_5H_{10}), 2.71 (br s, α-4H, C_5H_{10}), 6.83 (br s, 2H, NH_2), 7.04−7.84 (m, 55H, phenyl protons). $^{31}P\{^1H\}$ NMR ($CDCl_3$): *trans*-**11** δ 21.11 (d, $^2J_{P-P}$ = 3.4 Hz, $N(Ph_2PSe)_2$), 48.83 (m, PPh_3); *cis*-**11** δ 18.48, 21.96, 22.64, 27.25, 50.81 (all multiplets). IR (KBr; cm^{-1}): 3352-(w) [ν(N−H)], 1202(s) and 795(s) [$\nu(P_2N)$], 532(vs) [ν(P═Se)]. MS (FAB): *m*/*z* 1447 ($M^+ - C_5H_{10}NNH_2$). $E_{1/2}$ (CH_2Cl_2; V): −0.23 [Ru-(III/II)]. Anal. Calcd for $C_{71}H_{67}N_4P_5Se_4Ru$: C, 55.08; H, 4.36; N, 3.62. Found: C, 54.70; H, 4.39; N, 3.42.

Preparations of *cis*- and *trans*-Ru[N(Ph$_2$PQ)$_2$]$_2$(PPh$_3$)(NH$_2$NH$_2$) (Q = S (12), Se (13)). These complexes were prepared similarly to **7** by using excess 35% NH_2NH_2 in H_2O. Both were found to exist as their cis and trans forms in solutions. Yield of **12**: 20 mg, 21%. ^{1}H NMR ($CDCl_3$): δ 5.29 (br s, NH_2), 5.33 (br s, $RuNH_2$), 7.00−8.42 (m, phenyl protons). $^{31}P\{^1H\}$ NMR ($CDCl_3$): *trans*-**12** δ 37.87 (d, $^2J_{P-P}$ = 3.4 Hz, $N(Ph_2PS)_2$), 46.51 (m, PPh_3); *cis*-**12** δ 38.37, 38.77, 40.44, 46.50, 50.17 (all multiplets). IR (KBr; cm^{-1}): 3307(w), 3286(w) [ν-(N−H)], 1258(s), 1154(m) and 802(s) [$\nu(P_2N)$], 564(vs) [ν(P═S)]. MS (FAB): *m*/*z* 998 ($M^+ - N_2H_4 - PPh_3 + 1$). Anal. Calcd for $C_{66}H_{59}N_4P_5S_4Ru$: C, 61.43; H, 4.53; N, 4.34. Found: C, 60.98; H, 4.61; N, 4.36.

Yield of **13**: 74 mg, 72%. ^{1}H NMR ($CDCl_3$): δ 0.86 (br s, NH_2), 3.75 (br s, $RuNH_2$), 6.51−7.61 (m, phenyl protons). $^{31}P\{^1H\}$ NMR ($CDCl_3$): *trans*-**13** δ 42.07 (d, $^2J_{P-P}$ = 44 Hz, $N(Ph_2PSe)_2$), 89.51 (m, PPh_3); *cis*-**13** δ 18.56, 22.05, 22.76, 27.35, 48.45 (all multiplets). IR (KBr; cm^{-1}): 3358(m) [ν(N−H)], 1138(s) and 780(s) [$\nu(P_2N)$], 540-(vs) [ν(P═Se)]. MS (FAB): *m*/*z* 1449 ($M^+ - N_2H_4$), 1186 ($M^+ - N_2H_4 - PPh_3$). Anal. Calcd for $C_{66}H_{59}N_4P_5Se_4Ru$: C, 53.56; H, 4.02; N, 3.78. Found: C, 53.71; H, 4.03; N, 3.45.

Preparations of *cis*- and *trans*-Ru[N(Ph$_2$PS)$_2$]$_2$(PPh$_3$)(L) (L = *t*-BuNHNH$_2$ (14), C$_5$H$_{10}$NNH$_2$ (15)). The procedure for the synthesis of **12** was followed using **1** as the starting material to prepare **14** and **15**. Both complexes were found to exist as their cis and trans forms in solution.

Yield of **14**: 74%. ^{1}H NMR ($CDCl_3$): δ 1.42 (s, 9H, *t*-Bu), 2.39 (br s, NH), 4.82 (br s, $RuNH_2$), 6.86−7.76 (m, 55H, phenyl protons). $^{31}P\{^1H\}$ NMR ($CDCl_3$): *trans*-**14** δ 35.27 (d, $^2J_{P-P}$ = 6.2 Hz, $N(Ph_2PS)_2$), 78.96 (br m, PPh_3); *cis*-**14** δ 36.21, 37.67, 38.65, 41.15, 50.75, (all multiplets). IR (KBr; cm^{-1}): 3208(w), 3201(w) [ν(N−H)], 1172(s) and 802(s) [$\nu(P_2N)$], 564(vs) [ν(P═S)]. MS (FAB): *m*/*z* 1349 (M^+), 1260 ($M^+ - t$-$BuNHNH_2$), 998 ($M^+ - t$-$BuNHNH_2 - PPh_3 + 1$). $E_{1/2}$ (CH_2Cl_2; V): −0.14 [Ru(III/II)]. Anal. Calcd for $C_{70}H_{66}N_4P_5S_4Ru$: C, 60.61; H, 4.94; N, 4.16. Found: C, 59.68; H, 5.08; N, 4.10.

Yield of **15**: 82 mg, 68%. ^{1}H NMR ($CDCl_3$): δ 1.26 (d, $2H_\gamma$, C_5H_{10}), 1.63 (d, $4H_\beta$, C_5H_{10}), 2.60 (m, $4H_\alpha$, C_5H_{10}), 6.76 (br s, 2H, NH_2), 7.00−7.77 (m, 55H, phenyl protons). $^{31}P\{^1H\}$ NMR ($CDCl_3$): *trans*-**15** δ 36.23 (d, $^2J_{P-P}$ = 3.6 Hz, $N(Ph_2PS)_2$), 50.24 (m, PPh_3); *cis*-**15** δ 37.63, 37.88, 38.23, 39.96, 46.53, (all multiplets). IR (KBr; cm^{-1}): 3294(w) [ν(N−H)], 1199(s), 1170(m) and 796(s) [$\nu(P_2N)$], 564(vs) [ν(P═S)]. MS (FAB): *m*/*z* 1359 (M^+), 1260 ($M^+ - C_5H_{10}NNH_2$), 999 ($M^+ - C_5H_{10}NNH_2 - PPh_3 + 1$). $E_{1/2}$ (CH_2Cl_2; V): −0.16 [Ru(III/II)]. Anal. Calcd for $C_{71}H_{67}N_4P_5S_4Ru$: C, 58.32; H, 4.58; N, 3.66. Found: C, 58.65; H, 4.59; N, 3.32.

Reaction of 1 with Hydrazine Monohydrate. To a solution of **1** (0.10 g, 0.079 mmol) in THF (15 mL) was added hydrazine monohydrate (ca. 0.03 mL). The resulting clear solution was stirred at room temperature for 30 min and then evaporated to dryness. The resulting red residue was washed with Et_2O and dissolved in 8 mL of CH_2Cl_2, and the mixture was filtered. The red filtrate, layered with Et_2O, was left to stand at room temperature for 3 days. The red blocks (49 mg) and yellow powder (43 mg) that formed were separated manually and were characterized as *trans*-$Ru[N(Ph_2PS)_2]_2(NH_3)(H_2O)$ (**16**) and *cis*-$Ru[N(Ph_2PS)_2]_2(PPh_3)(NH_3)$ (**5**), respectively. Characterization data for **16** are as follows. ^{1}H NMR ($CDCl_3$): δ 1.55 (br s, 2H, H_2O), 2.60 (br s, 3H, NH_3), 6.86−7.88 (m, 40H, phenyl protons). $^{31}P\{^1H\}$ NMR ($CDCl_3$): δ 37.89 (d, $^2J_{P-P}$ = 2.5 Hz, $N(Ph_2PS)_2$). IR (KBr; cm^{-1}): 3422 (br m) [$\nu(H_2O)$], 3284(m) [ν(N−H)], 1238(s), 1140(s) and 807-(s) [$\nu(P_2N)$], 562(vs) [ν(P═S)]. MS (FAB): *m*/*z* 1032 (M^+), 1014 ($M^+ - H_2O - 1$), 998 ($M^+ - H_2O - PPh_3 - NH_3 + 1$). Anal. Calcd for $C_{48}H_{45}N_3OP_4S_4Ru$: C, 55.80; H, 4.39; N, 4.07. Found: C, 55.82; H, 4.16; N, 4.16.

Oxidation of 13 with Pb(OAc)$_4$. To a stirred solution of **13** (80 mg, 0.054 mmol) in CH_2Cl_2 (5 mL) at −78 °C was slowly added $Pb(OAc)_4$ (25 mg, 0.060 mmol) in CH_2Cl_2 (5 mL). There was a color change from orange to green upon warming the mixture to ambient temperature. The resulting solution was filtered, and the filtrate was

Table 1. Crystal Data and Structure Refinement Details for $Ru[N(Ph_2PSe)_2]_2(PPh_3)$ (**2**), *cis*-$Ru[N(Ph_2PSe)_2]_2(PPh_3)(NH_3)\cdot CH_2Cl_2$ (*cis*-**6**$\cdot CH_2Cl_2$), *cis*-$Ru[N(Ph_2PS)_2]_2(PPh_3)(t\text{-}BuNHNH_2)\cdot CH_2Cl_2$ (*cis*-**14**$\cdot CH_2Cl_2$), *cis*-$Ru[N(Ph_2PS)_2]_2(PPh_3)(C_5H_{10}NNH_2)$ (*cis*-**15**), and *trans*-$Ru[N(Ph_2PS)_2]_2(H_2O)(NH_3)$ (**16**)

	2	*cis*-**6**$\cdot CH_2Cl_2$	*cis*-**14**$\cdot CH_2Cl_2$	*cis*-**15**	**16**
empirical formula	$C_{66}H_{55}N_2P_5Se_4Ru$	$C_{67}H_{60}N_3Cl_2P_5Se_4Ru$	$C_{71}H_{68}N_4Cl_2P_5S_4Ru$	$C_{71}H_{67}N_4P_5S_4Ru$	$C_{48}H_{45}N_3OP_4S_4Ru$
fw	1447.88	1549.84	1432.35	1360.45	1033.11
crystal system	monoclinic	triclinic	triclinic	monoclinic	triclinic
space group	$P2_1/c$ (No. 14)	$P\bar{1}$ (No. 2)	$P\bar{1}$ (No. 2)	$P2_1/n$ (No. 14)	$P\bar{1}$ (No. 2)
a, Å	10.4401(5)	13.0385(6)	13.3573(7)	13.316(3)	10.7575(8)
b, Å	26.6189(13)	14.1278(6)	14.5662(8)	20.094(4)	14.1661(8)
c, Å	25.1173(12)	19.5468(8)	19.9542(11)	25.977(5)	18.4217(9)
α, deg		90.4100(10)	75.0820(10)		69.262(9)
β, deg	98.4580(10)	102.1260(10)	89.6690(10)	100.73(3)	86.401(9)
γ, deg		109.5790(10)	62.8650(10)		73.812(9)
V, Å^3	6904.3(6)	3305.0(2)	3310.4(3)	6829(2)	2519.3(4)
Z	4	2	2	4	2
ρ_{calcd}, g cm^{-3}	1.393	1.557	1.437	1.323	1.362
temp, °C	23	23	23	23	23
F(000)	2880	1544	1478	2816	1060
μ(Mo Kα), cm^{-1}	24.89	26.84	6.11	5.13	6.41
no. of data/restraints/params	15 388/0/703	14 269/0/740	14 281/0/785	15 237/0/767	6343/0/550
goodness-of-fit on F^2	0.903	1.009	0.944	1.145	1.35
R1	0.0353	0.0410	0.0557	0.0504	0.065
wR2 or R_w	0.1251[a]	0.1022[a]	0.1815[a]	0.1209[a]	0.063[b]

[a] wR2. [b] R_w.

concentrated to ca. 5 mL. Addition of diethyl ether led to the formation of a paramagnetic black powder. IR (KBr; cm^{-1}): 1205(m), 1151(s) and 796(s) [$\nu(P_2N)$], 533(vs) [ν(P═Se)].

Air Oxidation of 12. A CH_2Cl_2 (10 mL) solution of **12** (0.10 g, 0.077 mmol) was stirred under an atmosphere of dry air overnight at room temperature, during which the solution gradually turned green. The greenish-yellow mixture was filtered, and the filtrate was layered with hexane. Yellow crystals analyzed as $Ru[N(Ph_2PS)_2]_2(PPh_3)(N_2H_2)$ (**18**) were obtained in low yield (15 mg, 17%), along with a large amount of uncharacterized black precipitate. Characterization data for **18** are as follows: ^{1}H NMR ($CDCl_3$): δ 7.05−8.10 (m, phenyl protons); NH signals not detected. $^{31}P\{^1H\}$ NMR ($CDCl_3$): δ 36.65, 36.73, 40.56, 41.94, 50.17 (all multiplets). IR (KBr; cm^{-1}): 3341(w) and 3330(w) [ν(N−H)], 1572(m) [ν(N═N)], 1258(s) and 801(s) [$\nu(P_2N)$], 564(vs) [ν(P═S)]. MS (FAB): *m*/*z* 1260 ($M^+ - N_2H_2$), 998 ($M^+ - N_2H_2 - PPh_3 + 1$). Anal. Calcd for $C_{66}H_{57}N_4P_5S_4Ru\cdot CH_2Cl_2$: C, 58.56; H, 4.43; N, 4.02. Found: C, 59.14; H, 4.44; N, 3.86.

X-ray Crystallographic Studies. Single crystals of **2** (black-green), *cis*-**6**$\cdot CH_2Cl_2$ (orange-red), *cis*-**14**$\cdot CH_2Cl_2$ (orange), *cis*-**15** (orange), and **16** (red) were obtained by slow diffusion of diethyl ether into CH_2Cl_2 solutions of the complexes. Diffraction data for **2**, *cis*-**6**$\cdot CH_2Cl_2$, *cis*-**14**$\cdot CH_2Cl_2$, and *cis*-**15** were collected at room temperature on a Bruker SMART CCD area-detector diffractometer using graphite-monochromated Mo Kα radiation (λ = 0.710 73 Å). Cell parameters and orientation matrices for these structures were obtained from the least-squares refinements of reflections measured in three different sets of 15 frames each. The collected frames were processed with the software SAINT,[14a] and an absorption correction was applied (SADABS[14b]) to the collected reflections. Diffraction data for **16** were collected on a Rigaku ACF7R diffractometer with the use of graphite-monochromated Mo Kα radiation (λ = 0.710 73 Å). The structures were solved by direct methods in conjunction with standard difference Fourier techniques and subsequently refined by full-matrix least-squares analyses. All calculations were done by the program packages SHELXTL V5.0[15] (for **2**, *cis*-**6**$\cdot CH_2Cl_2$, *cis*-**14**, and *cis*-**15**) and TEXSAN[16] (for **16**). Non-hydrogen atoms for **2**, *cis*-**6**$\cdot CH_2Cl_2$, *cis*-**14**, and **16** were refined anisotropically. For *cis*-**14**$\cdot CH_2Cl_2$, three carbon atoms of one methyl group in the *tert*-butyl moiety were refined isotropically. Hydrogen atoms in the phenyl and other organic moieties were treated as idealized contributions except for the hydrogen atoms of H_2O and NH_3 in complex **16**, which were located by a difference Fourier synthesis based on low-angle data (θ < 15°) and refined. Crystallographic data and experimental details are listed in Table 1. Selected bond distances and angles for **2**, *cis*-**6**$\cdot CH_2Cl_2$, *cis*-**14**$\cdot CH_2Cl_2$, *cis*-**15**, and **16** are given in Tables 2−6, respectively.

Table 2. Selected Bond Lengths (Å) and Angles (deg) for $Ru[N(Ph_2PSe)_2]_2(PPh_3)$ (**2**)

Bond Lengths			
Ru(1)−Se(1)	2.5269(5)	Ru(1)−Se(2)	2.5410(5)
Ru(1)−Se(3)	2.4828(5)	Ru(1)−Se(4)	2.4561(5)
Ru(1)−P(5)	2.2025(11)	Se(1)−P(1)	2.1809(11)
Se(2)−P(2)	2.1835(11)	Se(3)−P(3)	2.1837(11)
Se(4)−P(4)	2.1946(12)		

Bond Angles			
Se(1)−Ru(1)−Se(2)	87.715(17)	Se(3)−Ru(1)−Se(4)	99.984(18)
Se(1)−Ru(1)−Se(4)	160.13(2)	Se(2)−Ru(1)−Se(3)	160.946(19)
Se(1)−Ru(1)−Se(3)	84.885(17)	Se(2)−Ru(1)−Se(4)	81.546(17)
P(5)−Ru(1)−Se(1)	92.05(3)	P(5)−Ru(1)−Se(2)	94.28(3)
P(5)−Ru(1)−Se(3)	103.50(3)	P(5)−Ru(1)−Se(4)	105.32(3)
P(1)−Se(1)−Ru(1)	95.48(3)	P(2)−Se(2)−Ru(1)	97.77(3)
P(3)−Se(3)−Ru(1)	112.72(3)	P(4)−Se(4)−Ru(1)	112.19(3)

Results and Discussion

Synthesis and Characterization of $Ru[N(Ph_2PSe)_2]_2(PPh_3)$. Treatment of $Ru(PPh_3)_3Cl_2$ with $K[N(Ph_2PSe)_2]$ in THF gave $Ru[N(Ph_2PSe)_2]_2(PPh_3)$ (**2**) as the sole isolable product. The KBr IR spectrum of **2** shows the $\nu(P_2N)$ bands at 1172(s) and 800(s) cm^{-1} and the ν(P═Se) band at 532(vs) cm^{-1}, reflecting the increase in P−N bond order and decrease in P═Se double-bond character for the $[N(Ph_2PSe)_2]^-$ ligand compared to its protonated form $HN(Ph_2PSe)_2$ [$\nu(P_2N)$ at 937, 926, and 918 cm^{-1}; ν(P═Se) at 595 and 546 cm^{-1}].[12b] The $^{31}P\{^1H\}$ NMR spectrum of **2** in $CDCl_3$ shows an intense singlet at δ 34.53 and a weak singlet at δ 23.19, assignable to $[N(Ph_2PSe)_2]^-$ and PPh_3, respectively. The ^{31}P resonant signal for $[N(Ph_2PSe)_2]^-$ in **2** (δ 34.5) is less downfield than that for $Ru[N(PPh_2S)_2]_2(PPh_3)$ (**1**) (δ 37.8). A similar trend has also been found for the related indium(III) (δ 33.2 for $In[N(Ph_2PS)_2]_3$ versus δ 28.5 for $In[N(Ph_2PSe)_2]_3$)[17] and yttrium(III) (δ 47.8 for $Cp_2Y[N(Ph_2PS)_2]$

(14) (a) *SAINT Reference Manual*; Siemens Energy and Automation Co.: Madison, WI, 1994−1996. (b) Sheldrick, G. M. *SADABS*: *Empirical Absorption Correction Program*; University of Göttingen: Göttingen, Germany, 1997.
(15) Sheldrick, G. M. *SHELXTL-Plus V5.1 Software Reference Manual*; Bruker AXS Inc.: Madison, WI, 1997.
(16) *TEXSAN*: *Crystal Structure Package*; Molecular Structure Corp.: Houston, TX, 1985 and 1992.

Table 3. Selected Bond Lengths (Å) and Angles (deg) for *cis*-Ru[N($Ph_2PSe)_2]_2(PPh_3)(NH_3)\cdot CH_2Cl_2$ (*cis*-**6**$\cdot CH_2Cl_2$)

Bond Lengths			
Ru(1)−Se(1)	2.5285(5)	Ru(1)−Se(2)	2.5225(5)
Ru(1)−Se(3)	2.6017(5)	Ru(1)−Se(4)	2.5389(5)
Ru(1)−P(5)	2.2778(11)	Ru(1)−N(3)	2.185(3)
Se(1)−P(1)	2.1784(11)	Se(2)−P(2)	2.1869(11)
Se(3)−P(3)	2.1620(11)	Se(4)−P(4)	2.1737(11)

Bond Angles			
Se(1)−Ru(1)−Se(2)	99.768(17)	Se(3)−Ru(1)−Se(4)	94.861(17)
Se(1)−Ru(1)−Se(4)	173.756(18)	Se(2)−Ru(1)−Se(3)	88.997(17)
Se(1)−Ru(1)−Se(3)	88.400(17)	Se(2)−Ru(1)−Se(4)	85.635(17)
P(5)−Ru(1)−Se(1)	86.71(3)	P(5)−Ru(1)−Se(2)	92.87(3)
P(5)−Ru(1)−Se(3)	174.99(3)	P(5)−Ru(1)−Se(4)	89.92(3)
N(3)−Ru(1)−Se(1)	80.89(8)	N(3)−Ru(1)−Se(2)	172.10(9)
N(3)−Ru(1)−Se(3)	83.15(9)	N(3)−Ru(1)−Se(4)	94.19(8)
N(3)−Ru(1)−P(5)	95.02(9)	P(1)−Se(1)−Ru(1)	111.09(3)
P(2)−Se(2)−Ru(1)	107.48(3)	P(3)−Se(3)−Ru(1)	109.15(3)
P(4)−Se(4)−Ru(1)	106.95(3)		

Table 4. Selected Bond Lengths (Å) and Angles (deg) for *cis*-Ru[$N(Ph_2PS)_2]_2(PPh_3)$(*t*-$BuNHNH_2)\cdot CH_2Cl_2$ (*cis*-**14**$\cdot CH_2Cl_2$)

Bond Lengths			
Ru(1)−S(1)	2.4205(10)	Ru(1)−S(2)	2.4051(10)
Ru(1)−S(3)	2.4276(11)	Ru(1)−S(4)	2.5159(10)
Ru(1)−P(5)	2.2845(10)	Ru(1)−N(3)	2.152(3)
N(3)−N(4)	1.451(8)	S(1)−P(1)	2.0173(14)
S(2)−P(2)	2.0110(14)	S(3)−P(3)	2.0115(14)
S(4)−P(4)	1.9917(14)		

Bond Angles			
S(1)−Ru(1)−S(2)	95.41(4)	S(3)−Ru(1)−S(4)	96.58(4)
S(1)−Ru(1)−S(4)	89.62(4)	S(2)−Ru(1)−S(3)	175.56(4)
S(1)−Ru(1)−S(3)	85.31(4)	S(2)−Ru(1)−S(4)	87.81(3)
P(5)−Ru(1)−S(1)	94.47(4)	P(5)−Ru(1)−S(2)	86.09(4)
P(5)−Ru(1)−S(3)	89.49(4)	P(5)−Ru(1)−S(4)	172.95(4)
N(3)−Ru(1)−S(1)	171.40(10)	N(3)−Ru(1)−S(2)	89.17(10)
N(3)−Ru(1)−S(3)	90.68(10)	N(3)−Ru(1)−S(4)	83.27(10)
N(3)−Ru(1)−P(5)	93.10(10)	Ru(1)−N(3)−N(4)	120.5(4)
P(1)−S(1)−Ru(1)	111.80(5)	P(2)−S(2)−Ru(1)	111.03(5)
P(3)−S(3)−Ru(1)	112.09(5)	P(4)−S(4)−Ru(1)	112.10(5)

Table 5. Selected Bond Lengths (Å) and Angles (deg) for *cis*-Ru[$N(Ph_2PS)_2]_2(PPh_3)(C_5H_{10}NNH_2)$ (*cis*-**15**)

BondLengths			
Ru(1)−S(1)	2.4947(10)	Ru(1)−S(2)	2.4312(10)
Ru(1)−S(3)	2.4474(9)	Ru(1)−S(4)	2.4051(10)
Ru(1)−P(5)	2.2991(10)	Ru(1)−N(3)	2.101(3)
N(3)−N(4)	1.405(5)	S(1)−P(1)	2.0051(14)
S(2)−P(2)	2.0055(13)	S(3)−P(3)	2.0108(13)
S(4)−P(4)	2.0093(13)		

BondAngles			
S(1)−Ru(1)−S(2)	90.45(4)	S(3)−Ru(1)−S(4)	94.45(4)
S(1)−Ru(1)−S(4)	92.16(3)	S(2)−Ru(1)−S(3)	81.96(4)
S(1)−Ru(1)−S(3)	87.42(4)	S(2)−Ru(1)−S(4)	175.46(3)
P(5)−Ru(1)−S(1)	177.69(3)	P(5)−Ru(1)−S(2)	91.54(4)
P(5)−Ru(1)−S(3)	91.70(4)	P(5)−Ru(1)−S(4)	85.77(3)
N(3)−Ru(1)−S(1)	89.99(9)	N(3)−Ru(1)−S(2)	89.88(8)
N(3)−Ru(1)−S(3)	171.42(8)	N(3)−Ru(1)−S(4)	93.82(8)
N(3)−Ru(1)−P(5)	91.19(9)	Ru(1)−N(3)−N(4)	129.0(2)
P(1)−S(1)−Ru(1)	111.44(5)	P(2)−S(2)−Ru(1)	110.62(5)
P(3)−S(3)−Ru(1)	112.75(5)	P(4)−S(4)−Ru(1)	111.46(5)

versus δ 41.03 for $Cp_2Y[N(Ph_2PSe)_2])$[18] systems. The positive-ion FAB mass spectrum of **2** shows the molecular ions {Ru-$[N(Ph_2PSe)_2]_2(PPh_3)\}^+$ and $\{Ru[N(Ph_2PSe)_2]_2\}^+$ with the characteristic isotopic distribution patterns.

The solid-state structure of **2** has been established by X-ray crystallography. Unlike the sulfide analogue **1**, which crystallizes

Table 6. Selected Bond Lengths (Å) and Angles (deg) for *trans*-Ru[$N(Ph_2PS)_2]_2(H_2O)(NH_3)$ (**16**)

BondLengths			
Ru(1)−S(1)	2.400(2)	Ru(1)−S(2)	2.402(2)
Ru(1)−S(3)	2.430(2)	Ru(1)−S(4)	2.411(2)
Ru(1)−O(1)	2.118(4)	Ru(1)−N(3)	2.142(6)
S(1)−P(1)	2.009(3)	S(2)−P(2)	1.981(3)
S(3)−P(3)	2.001(2)	S(4)−P(4)	2.017(2)

Bond Angles			
S(1)−Ru(1)−S(2)	100.42(7)	S(3)−Ru(1)−S(4)	101.43(6)
S(1)−Ru(1)−S(4)	170.75(7)	S(2)−Ru(1)−S(3)	172.18(7)
S(1)−Ru(1)−S(3)	78.93(6)	S(2)−Ru(1)−S(4)	80.48(7)
O(2)−Ru(1)−S(1)	93.9(1)	O(2)−Ru(1)−S(2)	85.3(1)
O(2)−Ru(1)−S(3)	87.0(1)	O(2)−Ru(1)−S(4)	95.3(1)
N(3)−Ru(1)−S(1)	85.4(2)	N(3)−Ru(1)−S(2)	93.8(2)
N(3)−Ru(1)−S(3)	93.9(2)	N(3)−Ru(1)−S(4)	85.3(2)
P(1)−S(1)−Ru(1)	111.53(9)	P(2)−S(2)−Ru(1)	110.9(1)
P(3)−S(3)−Ru(1)	109.11(9)	P(4)−S(4)−Ru(1)	109.43(9)
N(3)−Ru(1)−O(2)	178.8(2)		

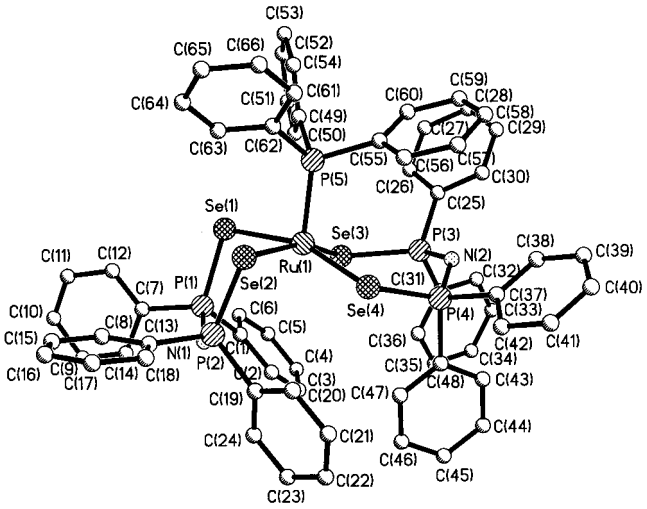

Figure 1. Perspective view of Ru[$N(Ph_2PSe)_2]_2(PPh_3)$ (**2**).

in the triclinic space group $P\bar{1}$,[10] complex **2** crystallizes in the monoclinic space group $P2_1/c$. An ORTEP diagram of the molecular structure of **2** is shown in Figure 1. Selected bond distances and angles are given in Table 2. The molecule is mononuclear with pseudo square pyramidal geometry. The terminal PPh_3 ligand occupies the apical position, and two chelating $[N(Ph_2PSe)_2]^-$ ligands form the basal plane. The six-membered $RuSe_2P_2N$ rings are nonplanar and severely distorted, displaying a twisted-boat conformation imposed by the non-parallel orientation of the two P−Se bonds in each ligand moiety. Each ring contains a pair of long and short Ru−Se bonds [Ru(1)−Se(2) = 2.5410(5) ("long") with Ru(1)−Se(1) = 2.5269(5) ("short"); Ru(1)−Se(3) = 2.4828(5) Å ("long") with Ru(1)−Se(4) = 2.4561(5) Å ("short")]. The average Ru−Se distance of 2.5017(5) Å in **2** is obviously longer than the average Ru−S distances of 2.401(2) and 2.3728(4) Å in **1**. The apical Ru−P bond length in **2** (2.2025(11) Å) is slightly shorter than that in **1** (2.220(2) Å).[10]

Pyridine Adducts of 1 and 2. Like **1**, **2** is a formally 16e complex and reacts with Lewis bases to give octahedral 18e adducts. Treatment of **2** in THF with excess pyridine (py) at room temperature resulted in an orange solution, indicating the formation of the adduct Ru[$N(Ph_2PSe)_2]_2(PPh_3)$(py) (**3**). The ^{31}P NMR spectrum shows a doublet at δ 22.45 for $[N(Ph_2PSe)_2]^-$ and a broad multiplet at δ 45.19 due to PPh_3, indicative of the trans geometry of the pyridine adduct. This is in contrast with the reaction of **1** with py, which yielded a mixture of the cis and trans products.[10] Recrystallization from CH_2Cl_2/hexane

(17) Cea-Olivares, R.; García-Montalvo, V.; Novosad, J.; Woollins, J. D.; Toscano, R. A.; Espinosa-Pérez, G. *Chem. Ber*. **1996**, *129*, 919.
(18) Pernin, C. G.; Ibers, J. A. *Inorg. Chem*. **1999**, *38*, 5478.

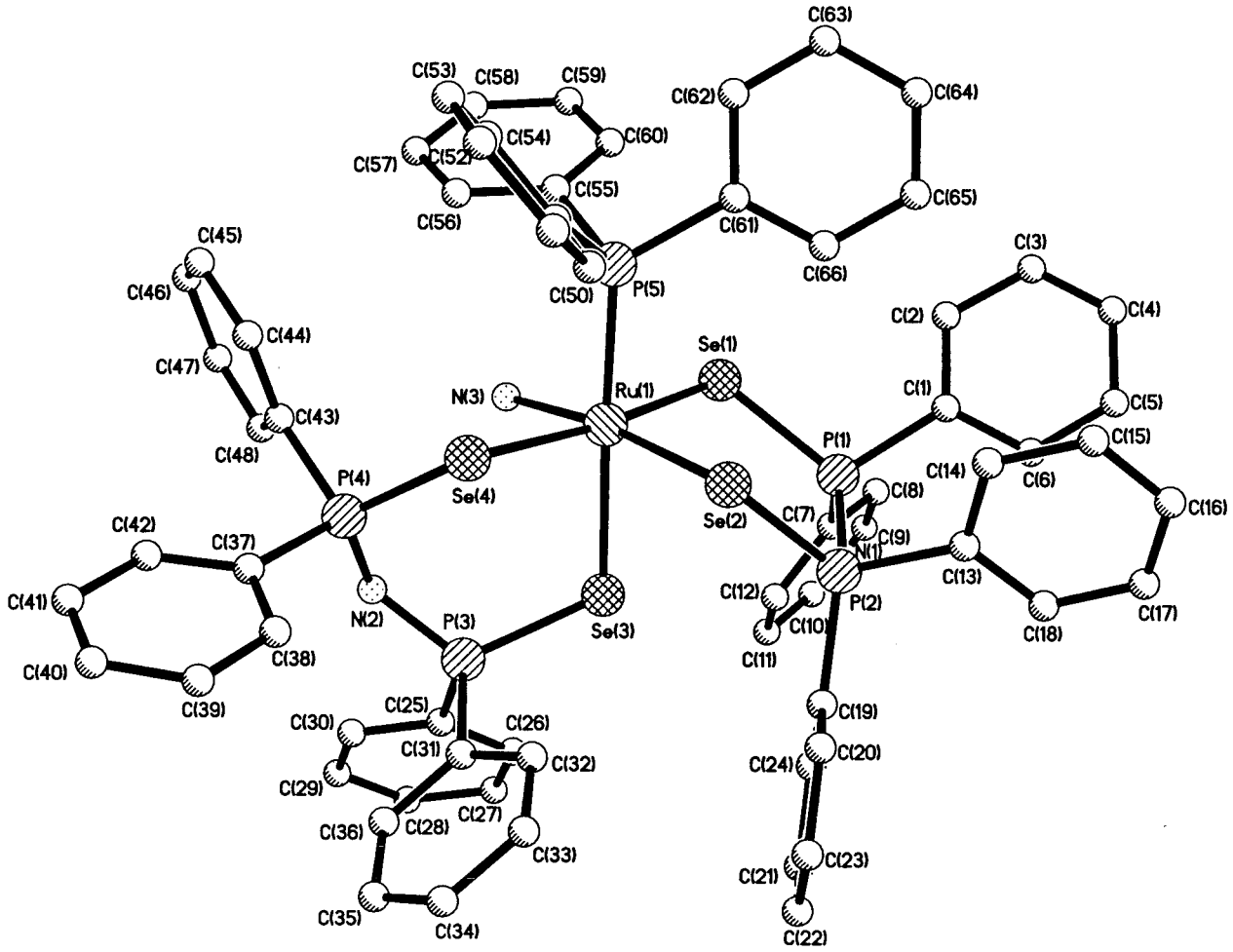

Figure 2. Perspective view of *cis*-Ru[N(Ph_2PSe)$_2$](PPh_3)(NH_3) (*cis*-**6**).

afforded analytically pure *trans*-**3**, isolated as air-stable orange needles. However, when a solution of *trans*-**3** in $CDCl_3$ was left to stand room temperature for hours, the intensity of the *trans*-**3** signals decreased gradually as five new ^{31}P signals appeared. These five signals were attributed to *cis*-**3** because a similar ^{31}P NMR spectral pattern has been observed for *cis*-Ru[N(Ph_2PS)$_2$]$_2$(PPh_3)(SO_2).[10] Therefore it appears that reaction of **2** with py initially gave the kinetic product *trans*-**3**, which crystallized from the reaction mixture. In solution, *trans*-**3** slowly isomerized to give the thermodynamic product *cis*-**3** (eq 1). On

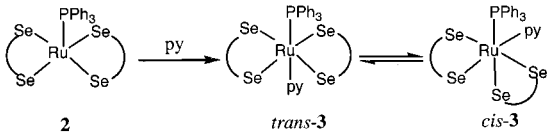

(1)

the basis of the integration of the py α proton signals, the equilibrium constant for *trans*-**3** ⇔ *cis*-**3** in $CDCl_3$ at room temperature was estimated to be approximately 1.67.

SO_2 Adducts of 1 and 2. As expected, electron-rich **2** has a high affinity for π-acid ligands. Thus, bubbling SO_2 gas into a THF solution of **2** led to the formation of the SO_2 adduct Ru[N(Ph_2PSe)$_2$]$_2$(PPh_3)(SO_2) (**4**), which was isolated as a mixture of the cis and trans isomers according to $^{31}P\{^1H\}$ NMR spectroscopy. This result contrasts with that of the corresponding reaction of **1** with SO_2, which yielded the structurally characterized cis product *cis*-Ru[N(Ph_2PS)$_2$]$_2$(PPh_3)(SO_2) only.[10] The difference in geometry between **4** and *cis*-Ru[N(Ph_2PS)$_2$]$_2$-(PPh_3)(SO_2) may be due to electronic (the Se donor is more electron-rich than S donor) and/or steric (the Ru−Se bond is longer than the Ru−S bond) factors, which are not well understood at this stage. It may also be possible that *trans*-**4** is the kinetic product of the reaction of **1** with SO_2, as in the formation of *cis*- and *trans*-**3**. The IR spectrum of **4** shows ν(S═O) signals at 1117 and 996 cm^{-1}, which are lower than those for $Ru(NH_3)_4(SO_2)Cl_2$ (1300 and 1130 cm^{-1})[19] and *cis*-Ru[N(Ph_2PS)$_2$]$_2$(PPh_3)(SO_2) (1286 and 1078 cm^{-1}),[10] consistent with the S-bound coordination mode of SO_2.

Ammonia Adducts of 1 and 2. Reactions of **1** and **2** with NH_3(g) led to the formation of the corresponding NH_3 adducts Ru[N(Ph_2PQ)$_2$]$_2$(PPh_3)(NH_3) (Q = S (**5**), Se (**6**)) (eq 2), which

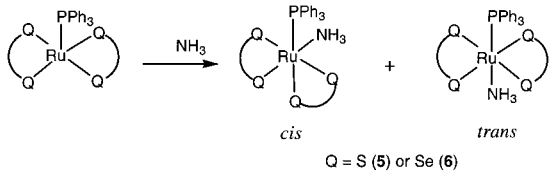

(2)

were characterized by elemental analyses and spectroscopic methods. Unlike the case of **3**, both the cis and trans forms of complexes **5** and **6** were observed in solution. The $^{31}P\{^1H\}$ NMR spectrum of **6** displays seven signals at δ 18.51 (m), 21.12 (d), 22.04 (m), 22.73 (m), 27.30 (m), 48.83 (m), and 51.64 (m). By comparison with the NMR data for *trans*-**3**, the signals at δ 21.12 (d) and 48.83 (m) were tentatively assigned to *trans*-**6**,

(19) Vogt, L. H.; Katz, J. L.; Wiberley, S. E. *J. Chem. Soc. A* **1965**, 1157.

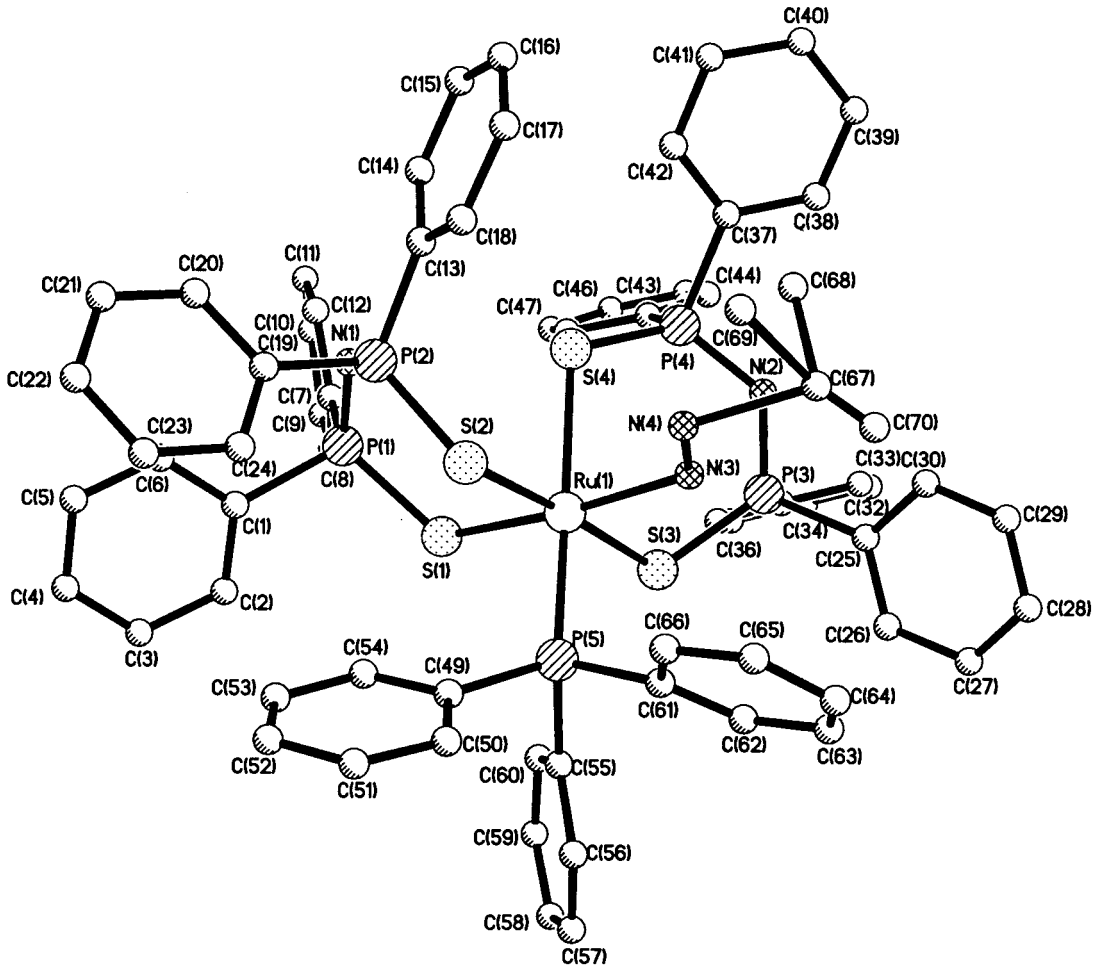

Figure 3. Perspective view of *cis*-Ru[$N(Ph_2PS)_2]_2(PPh_3)$(*t*-BuNHNH$_2$) (*cis*-**14**).

while the remaining five signals were assigned to *cis*-**6**. The ^{31}P resonant signals for *trans*-**5** (δ 37.89 for $[N(Ph_2PS)_2]^-$ and δ 46.53 for PPh_3) and *cis*-**5** (δ 36.14, 38.58, 38.92, 40.56, 50.28) were assigned similarly. The P−P coupling constants were not determined owing to the poor resolution of the signals. On the basis of integration of the NH_3 protons, the cis:trans ratio for the sample of **6** was determined to be ca. 1.85. The IR spectrum of **6** displays the diagnostic ν(N−H) signal at 3336 cm^{-1} along with the P═Se stretching vibration at 532 cm^{-1}. The P═S stretching vibration mode for **5** was found at 565 cm^{-1}. The identity of *cis*-**6** was confirmed by the X-ray crystallographic analysis. A perspective view of *cis*-**6** is depicted in Figure 2; selected bond lengths and angles are given in Table 3. The crystal lattice of **6** was found to contain a CH_2Cl_2 molecule filling a void. The geometry around the Ru atom is distorted octahedral with PPh_3 and NH_3 mutually cis. The bite angles Se(1)−Ru(1)−Se(2) (99.768(17)°) and Se(3)−Ru(1)−Se(4) (94.861(17)°) for the $RuSe_2P_2N$ rings in *cis*-**6**·CH_2Cl_2 are comparable to those in **2** and other $[N(Ph_2PSe)_2]^-$ complexes, for example, 101.27(3)° in $Pd(C_9H_{12}N)[N(Ph_2PSe)_2]$ and 99.3(1)° in $Pt[N(Ph_2PSe)_2]_2$.[20] The N−Ru−P angle of 95.02(9)° deviates by more than 5° from 90° owing to the steric repulsion between PPh_3 and NH_3, which also results in an elongation of the Ru−P bond from 2.2025(11) Å in **2** to 2.2778(11) Å in *cis*-**6**·CH_2Cl_2. The Ru−N distance for *cis*-**5**·CH_2Cl_2 (2.185(3) Å) agrees well with those in $[Ru(NH_3)_5(Me_2SO)](PF_6)_2$ (2.2169 Å)[21] and **16** (2.2142(6) Å; see later). The Ru−Se distances in *cis*-**6**·CH_2Cl_2 are in the range 2.5225(5)−2.6017(5) Å, comparable to those in **1** and $Ru_4(\mu\text{-Se})_2(\mu\text{-CO})(CO)_8[HN(PPh_2)_2]$ (2.552(2)-2.579(2) Å).[9]

Hydrazine and Hydroxylamine Adducts of 1 and 2. The success in isolating pyridine and ammonia adducts of **1** and **2** prompted us to prepare the hydrazine and hydroxylamine analogues. Treatment of **1** with excess 35% aqueous hydrazine afforded the hydrazine adduct $Ru[N(PPh_2S)]_2(PPh_3)(N_2H_4)$ (**12**) (eq 3), which was found to exist in both the cis and trans forms

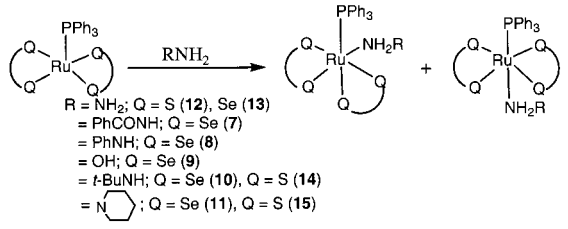

(3)

in solution. On the other hand, reaction of **2** with excess 35% aqueous hydrazine afforded yellow *trans*-**13** as the sole isolated product. Recrystallization of *trans*-**13** from CH_2Cl_2/E_2O resulted in isomerization and the formation of an orange-red crystalline product characterized as *cis*-**13**. Unfortunately, we were unable to obtain single crystals of *cis*-**13** for an X-ray diffraction study. Similarly, treatment of **2** and **3** with substituted hydrazines L and with NH_2OH yielded the respective adducts $Ru[N(Ph_2PQ)_2]_2(PPh_3)(L)$ (Q = S, L = *t*-BuNHNH$_2$ (**14**), $C_5H_{10}NNH_2$

(20) Bhattacharyya, P.; Slawin, A. M. Z.; Smith, M. B. *J. Chem. Soc., Dalton Trans.* **1998**, 2467.

(21) March, F. C.; Ferguson, G. *Can. J. Chem.* **1971**, *49*, 3590.

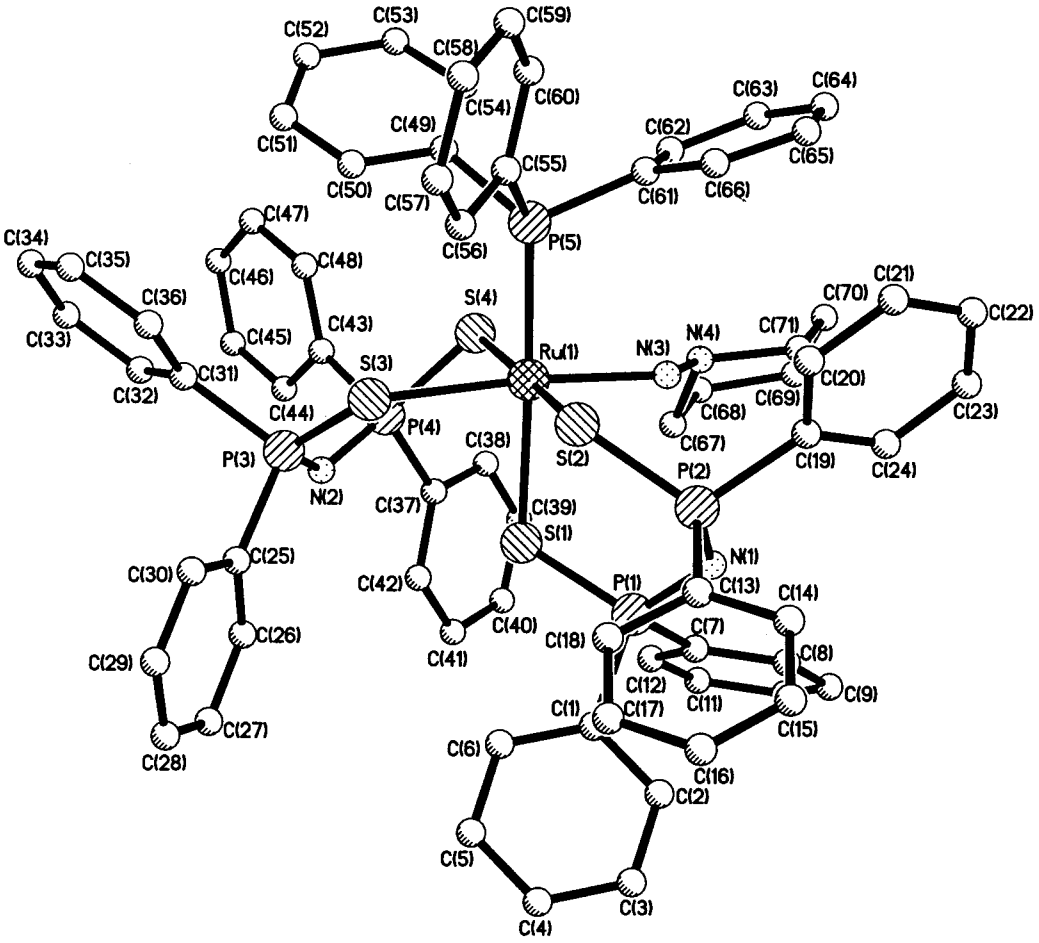

Figure 4. Perspective view of *cus*-Ru[$N(Ph_2PS)_2]_2(PPh_3)(C_5H_{10}NNH_2)$ (*cis*-**15**).

(**15**); Q = Se, L = $PhCONHNH_2$ (**7**), $PhNHNH_2$ (**8**), NH_2OH (**9**), *t*-$BuNHNH_2$ (**10**), $C_5H_{10}NNH_2$ (**11**)), which were isolated as mixtures of their trans and cis isomers. The reaction rates for the formation of the hydrazine adducts were found to be dependent on the substituents on hydrazine.[22] Thus, reactions of **1** and **2** with electron-rich NH_2OH, 1-aminopiperidine ($C_5H_{10}NNH_2$), and *t*-$BuNHNH_2$ were complete in ca. 15 min whereas longer reaction times (ca. 1 h) were needed for $PhCONHNH_2$ and $PhNHNH_2$. Complexes **7**−**15** are air-sensitive orange or red-orange crystalline solids. They are soluble in polar organic solvents such as CH_2Cl_2 and DMF, in which they behave as nonconductors. The IR spectra of **8**−**15** display characteristic ν(N−H) bands in the 3210−3340 cm^{-1} region. The IR spectrum of **7** displays ν(N−H) bands at 3211 and 3227 cm^{-1}, along with an intense ν(C═O) signal at 1632 cm^{-1}, which is lower than that for free $PhCONHNH_2$ (1665 cm^{-1}). For complexes **7**, **8**, **10**, and **14**, the hydrazine NH_2 and NH resonant signals appear as two broad singlets, which integrate accurately in a ratio of 1:2. For complexes **12** and **13**, two nonequivalent NH signals are observed, indicating that these complexes are mononuclear and that the hydrazine binds to Ru in an η^1 fashion. The $^{31}P\{^1H\}$ NMR spectra of complexes **7**−**11**, **14**, and **15** each show seven signals, indicative of the presence of the trans and cis isomers for these complexes in solution.

The course of reaction between **2** and hydrazine was followed by ^{31}P NMR spectroscopy. Treatment of **2** with a slight excess of 35% aqueous hydrazine in $CDCl_3$ initially yielded yellow trans-**13** (δ 42.07 and 89.51 due to $[N(Ph_2PSe)_2]^-$ and PPh_3, respectively). After the solution was allowed to stand for 1 day at room temperature, five additional ^{31}P signals attributable to *cis*-**13** appeared. Thus, it appears that, as in the formation of the pyridine adduct, *trans*-**13** was the kinetic product while *cis*-**13** was the thermodynamic product for the reaction between **2** and hydrazine. The yield of *trans*-**13** was enhanced if a large excess of hydrazine was used. Recrystallization of **13** from CH_2Cl_2/hexane afforded orange crystals of pure *cis*-**13**, along with a yellow powder, presumably containing *trans*-**13**, which has not yet been isolated in a pure form.

X-ray-quality single crystals of *cis*-**14**·CH_2Cl_2 and *cis*-**15** were easily obtained by recrystallization of the complexes from CH_2Cl_2/E_2O. Their solid-state structures were then established by X-ray crystallography. The molecular structures of *cis*-**14** and *cis*-**15** are shown in Figures 3 and 4, respectively. Tables 4 and 5 list the selected bond distances and angles for *cis*-**14**·CH_2Cl_2 and *cis*-**15**, respectively. For both structures, the geometry around Ru is pseudooctahedral with PPh_3 cis to the hydrazine ligand. The Ru−N bond lengths in *cis*-**14**·CH_2Cl_2 (2.152(3) Å) and *cis*-**15** (2.101(3) Å) are consistent with an Ru−N(sp^3) dative bond. The Ru−N−N bond angles in *cis*-**14**·CH_2Cl_2 (120.5(4)°) and *cis*-**15** (129.0(2)°) are somewhat opened compared to the tetrahedral value. The Ru−N−N angle in *cis*-**15** is larger than that in *cis*-**13**·CH_2Cl_2, possibly due to the steric bulk of the piperidine moiety. For this reason, the N−N bond length (1.451(8) Å) for *cis*-**14**·CH_2Cl_2 is slightly longer than that for *cis*-**15** (1.405(2) Å). The N−N bond lengths for both complexes are comparable to that for $[(\eta^6\text{-}C_6Me_6)Ru(S\text{-}2,6\text{-}C_6H_3Me_2)_2(NH_2NH_2)]$ (1.378(10) Å),[23] indicating that the N−N bond is a single bond. It is noteworthy that the Ru−P bond lengths in *cis*-**14**·

(22) Albertin, G.; Antoniutti, S.; Bacchi, A.; Bordignon, E.; Dolcetti, P. M.; Pelizzi, G. *J. Chem. Soc., Dalton Trans.* **1997**, 4435.

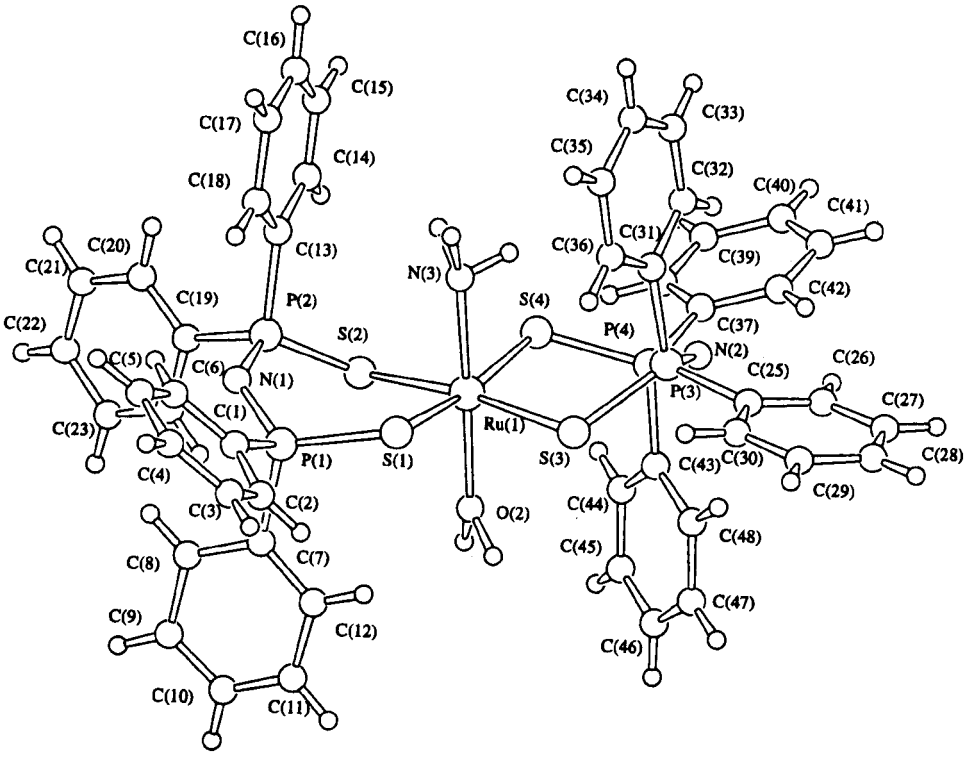

Figure 5. Perspective view of *trans*-Ru[$N(Ph_2PS)_2]_2(NH_3)(H_2O)$ (**16**).

CH_2Cl_2 (2.2845(10) Å) and *cis*-**15** (2.2991(10) Å) are somewhat longer than that found in **1** (2.220(2) Å).[10] This elongation may be due to the steric bulk and/or electron-donating properties of the coordinated *t*-$BuNHNH_2$ and $C_5H_{10}NNH_2$ ligands. The Ru−S bond lengths for the two complexes are normal by comparison with other related complexes in the literature.[8,10,24]

Reaction of 1 with hydrazine monohydrate. Interestingly, treatment of **1** with hydrazine monohydrate ($N_2H_4{\cdot}H_2O$) led to the isolation of yellow *cis*-Ru[$N(Ph_2PS)_2]_2(PPh_3)(NH_3)$ (*cis*-**5**) and red *trans*-Ru[$N(Ph_2PS)_2]_2(NH_3)(H_2O)$ (**16**) eq 4), which

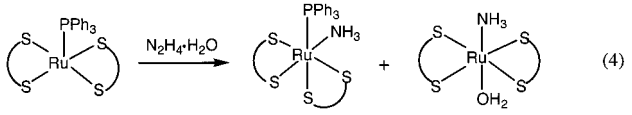

1 *cis*-**5** **16** (4)

were characterized by mass spectrometry, ^1H NMR spectroscopy, and elemental analyses. The ammine ligands in *cis*-**5** and **16** apparently came from the hydrazine hydrate (either via a redox reaction of hydrazine or from the ammonia impurity in hydrazine). It may be noted that 1e reduction of hydrazine to give NH_3 or NH_4^+ and metal-mediated decomposition of hydrazine to give metal ammine complexes are well documented.[25] The difference in reactivity toward **1** between aqueous hydrazine and hydrazine hydrate may be due to a concentration effect. The IR spectrum of **16** shows a broad band at 3422 cm^{-1} and a weak band at 3284 cm^{-1}, which were assigned as the O−H and N−H stretches, respectively. The solid-state structure of **16** was established by X-ray crystallography. Figure 5 shows a perspective view of **16**; selected bond lengths and angles are listed in Table 6. The ruthenium center has an octahedral coordination environment with the NH_3 and H_2O ligands mutually trans. The bite angles S(1)−Ru(1)−S(2) and S(3)−Ru(1)−S(4) in **16** are substantially larger than those in *cis*-**14**·CH_2Cl_2 and *cis*-**15**. The Ru−S bond lengths in **16** agree well with those in *cis*-**14**·CH_2Cl_2 and *cis*-**15**. The Ru−O bond distance 2.118(4) Å is similar to that observed for [RuTp(H_2O)-$(P(i\text{-}Pr_2)Me)_2$](OTf) [2.142(6) Å; Tp = hydrotris(pyrazolyl)-borate].[26] The Ru−N bond distance of 2.142(6) Å is in the normal range for a Ru−N single bond.

Electrochemistry. Formal potentials of the $Ru^{II}[N(Ph_2PQ)_2]$ complexes were determined by cyclic voltammetry. The cyclic voltammogram of **2** in CH_2Cl_2 shows a reversible couple at $E_{1/2}$ = −0.17 V vs $Cp_2Fe^{+/0}$, which was assigned as the metal-centered Ru(III/II) couple because $HN(Ph_2PSe)_2$ is redox inactive at this potential. It is quite surprising that the Ru(III/II) potential for **2** is similar to that for the sulfide analogue **1** (−0.24 V) because one might expect that selenide is a better π-donor than sulfide and thus should be more capable of stabilizing the Ru(III) state. The Ru(III/II) couple for the pyridine adduct **3** occurs at $E_{1/2}$ = −0.21 V, while those for the ammine and hydrazine adducts of **2** were found in the range of −0.19 to −0.28 V, indicating that the Ru(III) states for these complexes are stabilized by coordination to N-donor ligands. No Ru(III/II) oxidation was found for the SO_2 complex **4** because the Ru(II) state is stabilized by strongly π-acidic SO_2 ligand.

Oxidation of Ru(II) Hydrazine Complexes. Oxidation of the hydrazine ligand to give 1,2-diazene (NH═NH) complexes is well documented.[5,6] Sellmann and co-workers reported the preparations of the diazene complexes [(μ-NHNH){Fe(PR_3)-('S_4')}$_2$] (R = Me, Et, Ph) and [{Ru('S_4')(PPh_3)}$_2$(μ-NHNH)] ('S_4' = $[(SC_6H_4SCH_2)_2NH]^{2-}$) by air oxidation of the corre-

(23) Mashima, K.; Kaneyoshi, H.; Kaneko, S.; Tani, K.; Nakamura, A. *Chem. Lett*. **1997**, 569.
(24) (a) Maiti, R.; Shang, M.; Lappin, A. G. *Chem. Commun*. **1999**, 2349. (b) Kawano, M.; Uemura, H.; Watanabe, T.; Matsumoto, K. *J. Am. Chem. Soc*. **1993**, *115*, 2068.
(25) (a) Pickett, C. J. *J. Biol. Inorg. Chem*. **1996**, *1*, 601. (b) Sellmann, D.; Sutter, J. *J. Biol. Inorg. Chem*. **1996**, *1*, 587. (c) Stanbury, D. M. *Prog. Inorg. Chem*. **1998**, *47*, 511.
(26) Tenorio, M. A. J.; Tenorio, M. J.; Puerta, M. C.; Valerga, P. *J. Chem. Soc., Dalton Trans*. **1998**, 3601.

sponding hydrazine precursors.[6] Hillhouse and co-workers successfully isolated diazene complexes of Os(II) and W(II) by $Pb(OAc)_4$ oxidation of the corresponding hydrazine complexes at low temperature (−78 °C).[5] However, an attempt to prepare a ruthenium(II) diazene complex by Pb(IV) oxidation of **13** under similar reaction conditions led to the isolation of an intractable paramagnetic dark solid. The IR spectrum of this dark solid displayed characteristic bands for $[N(Ph_2PSe)_2]^-$ and PPh_3, but neither ν(N−H) nor ν(N═N) was observed. When a solution of **12** in CH_2Cl_2 was left to stand in air overnight, a yellow-green solution resulted. Slow evaporation of the yellow-green solution yielded an orange crystalline product analyzed as $Ru[N(Ph_2PS)_2](PPh_3)(N_2H_2)$ (**18**) along with an uncharacterized dark green paramagnetic species. The IR spectrum of **18** displays ν(N−H) signals at 3341 and 3330 cm^{-1}, which are slightly higher than those for **12**, along with a band at 1572 cm^{-1} assignable to ν(N═N). The solid-state structure of **18** was determined and was found to be consistent with the formulation of an Ru−NH═NH species.[27] However, because of disorder in the crystal structure, the proposed diazene formulation for **18** could not be definitively confirmed.

Summary

We synthesized a series of hydrazine complexes of ruthenium(II) in sulfur- and selenium-rich coordination environments. NMR spectroscopy revealed that these complexes exist as a mixture of their cis and trans isomers in solution. The products of the reactions between $Ru[N(Ph_2PQ)_2]_2(PPh_3)$ and hydrazine were found to be dependent on the nature of the hydrazine reagent used. Treatment of **2** with 35% aqueous hydrazine gave a ruthenium hydrazine complex, while **2** reacted with hydrazine hydrate to give a mixture of ruthenium(II) ammine phosphine and ammine aquo complexes. We believe that the chemistry of dinitrogen, diazene, and hydrazine coordinated to ruthenium is extensive and will provide further insights into the mechanism of abiological nitrogen fixation. Investigations in this area are under way.

Acknowledgment. We thank The Croucher Foundation and The Hong Kong University of Science and Technology for support.

Supporting Information Available: X-ray crystallographic files, in CIF format, for the structure determinations of **2**, *cis*-**6**·CH_2Cl_2, *cis*-**14**·CH_2Cl_2, *cis*-**15**, **16**, and **18**. This material is available free of charge via the Internet at http://pubs.acs.org.

IC000291C

(27) The solid-state structure of complex **18** is consistent with the formulation of the Ru(II) diazene species *cis*-$Ru[N(Ph_2PS)_2](PPh_3)(NH═NH)$. Crystal data for **18**, $C_{66}H_{59}N_4P_5S_4Ru$: $a = 10.663(8)$ Å, $b = 28.496(6)$ Å, $c = 20.446(4)$ Å, $\beta = 102.48(3)°$, $V = 6065(3)$ Å^3, monoclinic, $P2_1/n$ space group, $Z = 4$, $\rho_{calcd} = 1.413$ g cm^{-3}, $\mu = 5.73$ cm^{-1}, no. of data = 8137, $R = 0.068$, $R_w = 0.081$. The uncoordinated nitrogen N(4) of the N_2H_2 ligand was found to be 50:50 disordered. The observed average Ru−N(3)−N(4) angle of 134° is larger than those for hydrazine complexes *cis*-**14** and *cis*-**15** but is comparable to that for known diazene complexes such as $[Os(NH═NH)(CO)_2(PPh_3)_2Br][OTf)]$ (135.9(10)°).[5c] The Ru−N(3) and average N(3)−N(4) distances are 2.07(2) and 1.235 Å, respectively.